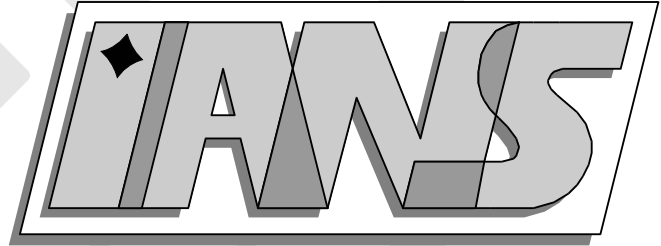


**Universität
Stuttgart**



Global existence and numerical simulations for a
reaction-diffusion system modeling pattern formation
on seashells

Jan Kelkel, Christina Surulescu

**Berichte aus dem Institut für
Angewandte Analysis und Numerische Simulation**

Preprint 2008/006

Universität Stuttgart

Global existence and numerical simulations for a
reaction-diffusion system modeling pattern formation
on seashells

Jan Kelkel, Christina Surulescu

**Berichte aus dem Institut für
Angewandte Analysis und Numerische Simulation**

Preprint 2008/006

Institut für Angewandte Analysis und Numerische Simulation (IANS)
Fakultät Mathematik und Physik
Fachbereich Mathematik
Pfaffenwaldring 57
D-70 569 Stuttgart

E-Mail: ians-preprints@mathematik.uni-stuttgart.de

WWW: <http://preprints.ians.uni-stuttgart.de>

ISSN **1611-4176**

© Alle Rechte vorbehalten. Nachdruck nur mit Genehmigung des Autors.
IANS-Logo: Andreas Klimke. \LaTeX -Style: Winfried Geis, Thomas Merkle.

GLOBAL EXISTENCE AND NUMERICAL SIMULATIONS FOR A REACTION-DIFFUSION SYSTEM MODELING PATTERN FORMATION ON SEASHELLS

J. KELKEL & C. SURULESCU

ABSTRACT. We investigate a reaction-diffusion system proposed by H. Meinhardt as a model for pattern formation on seashells. We prove the existence of a local solution for general initial conditions and parameters upon using an iterative approach. Furthermore, a global solution is shown to exist for suitable initial data. The behaviour of the solution in time and space is illustrated through numerical simulations.

1. INTRODUCTION

In nature a huge variety of patterns is encountered, on animal coats, on plants, in a cell population or in interacting chemicals during an industrial process. Pigment patterns on the shells of molluscs are among the most fascinating ones, due to their beauty and their great diversity, even within the same species. This latter fact is particularly interesting, since the patterns on these animals seem to have no functional significance, thus offering no evolutionary advantage. Though they look very different, it is however reasonable to expect that patterns are generated by similar molecular mechanisms.

Pattern formation is a phenomenon based on the interaction of different components, possibly under the influence of their surroundings. In his seminal work [13] Turing has shown that under certain conditions two interacting chemical species with different diffusion rates can generate a stable inhomogeneous pattern. Later Gierer and Meinhardt [2] and Segel and Jackson [10] have evidenced that the concepts of autocatalysis and long-range inhibition play an essential role. The models developed to explain pattern formation involve reaction-diffusion equations, where the reaction terms characterize the chemical interactions eventually generating the pattern. With adequate choices of these terms, the models were able to describe many patterns in great detail, even the filigree ones on molluscs [6].

The works of Meinhardt et al. [6], [5] are concerned with modeling of patterns on seashells and their computer simulations, as well as their interpretation in the framework of biochemical processes. Another direction is to investigate the

Date: June 2nd 2008.

Key words and phrases. pattern formation, reaction-diffusion equations.

Gierer-Meinhardt system for patterns on molluscs [2] from a qualitative viewpoint with the aid of dynamical systems methods, see e.g., [14], [15] and [4]. In [14] and [15] it is shown that the respective reaction-diffusion system is able to describe under certain conditions the generation of a special kind of patterns, the so-called spikes, while in [4] is evidenced the possibility of time oscillations. The existence of solutions to reaction-diffusion systems has also attracted considerable interest. Thus, Rothe [8] proved the existence of a global solution based on the method of semigroups of operators and later his result was further improved. A newer result on global solutions to the Gierer-Meinhardt system can be found in [3].

In this paper we consider a model proposed by Gierer and Meinhardt [2] for describing pattern formation on seashells through the interconditioning of two substances: an activator and an inhibitor. The first influences the production of the melanin pigment and -by autocatalysis- its own production, but also stimulates the creation of inhibitor, a chemical controlling the activator production.

After an outline of the stability analysis for the resulting reaction-diffusion system in Section 3, we give in Section 4 a new, simpler proof based on an iterative approach for the existence of a local in time weak solution to these equations. Then we show in Section 5 that the solution exists globally and finally perform numerical simulations in Section 6, to illustrate the space-time behavior of the solution.

2. PROBLEM SETTING

In the following, we deal with a system of partial differential equations for two functions $u, v : [0, T] \times \Omega \rightarrow \mathbb{R}$ modeling the concentration of activator, respectively inhibitor at the position $\mathbf{x} \in \Omega$ and time $t \in [0, T]$. Here $\Omega \subset \mathbb{R}^N$ ($N = 1, 2$) is a regular enough domain and $T > 0$. The partial differential equations describing the interaction between activator and inhibitor concentrations read

$$(1) \quad \frac{\partial u(t, \mathbf{x})}{\partial t} = d_u \Delta u(t, \mathbf{x}) + f(u(t, \mathbf{x}), v(t, \mathbf{x})), \quad (t, \mathbf{x}) \in (0, T) \times \Omega$$

and

$$(2) \quad \frac{\partial v(t, \mathbf{x})}{\partial t} = d_v \Delta v(t, \mathbf{x}) + g(u(t, \mathbf{x}), v(t, \mathbf{x})), \quad (t, \mathbf{x}) \in (0, T) \times \Omega.$$

The reaction functions $f(u, v)$ and $g(u, v)$ can be derived from chemical kinetics using the law of mass action (cf. [7]) and are given by

$$(3) \quad f(u, v) = \frac{s_1}{v(1 + S_u u^2)} u^2 + s_1 b_u - r_u u$$

and

$$(4) \quad g(u, v) = s_2 u^2 + b_v - r_v v.$$

The constants d_u and d_v are diffusion coefficients, s_1 and s_2 are production rates, r_u and r_v are rates of decay, and b_u and b_v are production rates for the activator, respectively the inhibitor. S_u is a coefficient indicating the saturation level in the system.

We assume that there is no exchange of the two chemicals with the environment:

$$(5) \quad \frac{\partial u}{\partial \boldsymbol{\nu}} = \frac{\partial v}{\partial \boldsymbol{\nu}} = 0 \quad \text{on } (0, T) \times \partial\Omega,$$

where $\boldsymbol{\nu}$ is the outward pointing normal vector on the boundary of Ω . The initial data is given by

$$(6) \quad u(0, \mathbf{x}) = u_0(\mathbf{x}), \quad v(0, \mathbf{x}) = v_0(\mathbf{x}) \quad \text{in } \Omega.$$

Here u_0 and v_0 are positive functions, satisfying the condition

$$\frac{\partial u_0}{\partial \boldsymbol{\nu}} = \frac{\partial v_0}{\partial \boldsymbol{\nu}} = 0 \quad \text{on } \partial\Omega.$$

3. STABILITY ANALYSIS

In this section we outline the qualitative properties of the Gierer-Meinhardt system in Section 2.

Using the following scalings (L denotes a characteristic length)

$$\tilde{u} = \frac{s_2}{s_1}u, \quad \tilde{v} = \frac{r_v s_2}{s_1^2}v, \quad \tilde{t} = \frac{d_u t}{L^2}, \quad \tilde{x}_i = \frac{x_i}{L}$$

and with the notations

$$\tilde{a} = \frac{b_u s_2}{r_v}, \quad \tilde{b} = \frac{r_u}{r_v}, \quad \tilde{c} = \frac{b_v s_2}{s_1^2}, \quad \tilde{d} = \frac{d_v}{d_u}, \quad \tilde{S}_u = \frac{s_1^2}{s_2^2}S_u, \quad \tilde{\gamma} = \frac{L^2 r_v}{d_u},$$

the equations can be rewritten (we omit the tildes in the new, dimensionless variables):

$$(7) \quad \frac{\partial u(t, \mathbf{x})}{\partial t} = \Delta u(t, \mathbf{x}) + \gamma f(u, v)$$

$$(8) \quad \frac{\partial v(t, \mathbf{x})}{\partial t} = d \Delta v(t, \mathbf{x}) + \gamma g(u, v),$$

with the reaction functions

$$(9) \quad f(u, v) = a - bu + \frac{u^2}{v(1 + S_u u^2)}$$

$$(10) \quad g(u, v) = u^2 - v + c.$$

As before, we assume initial conditions (6) and boundary conditions (5). The emergence of patterns essentially depends on the parameters of the above systems and on the form of the reaction terms. For instance, γ is proportional to the

size of the domain of interest; its influence will be illustrated in Section 6. For more details we refer to Section 2.2 in [7].

Following the lines of Section 2.3. in [7], we can characterize the Turing space, i.e. the set of parameter values for which there is diffusion driven instability in the system. In order for the latter to occur, the following conditions have to be satisfied:

$$\begin{aligned} v &= u^2 + c, & a &= bu + \frac{u^2}{(u^2 + c)(1 + S_u u^2)}, \\ \frac{\partial f}{\partial u} + \frac{\partial g}{\partial v} &< 0, & \frac{\partial f}{\partial u} \frac{\partial g}{\partial v} - \frac{\partial f}{\partial v} \frac{\partial g}{\partial u} &> 0, \\ d \frac{\partial f}{\partial u} + \frac{\partial g}{\partial v} &> 0 & \text{thus } d &\neq 1, \\ \left(d \frac{\partial f}{\partial u} + \frac{\partial g}{\partial v} \right)^2 &> 4 \left(\frac{\partial f}{\partial u} \frac{\partial g}{\partial v} - \frac{\partial f}{\partial v} \frac{\partial g}{\partial u} \right). \end{aligned}$$

Additionally to the spatial patterns, the Gierer-Meinhardt System may give rise to temporal oscillations. Applying the result in [4], a stable limit cycle exists for certain values of the reaction parameters:

Theorem 3.1. *If the parameters of the Gierer-Meinhardt system (1)-(6) without diffusion (i.e. $d_u = d_v = 0$) with $b_v = 0$ and $S_u = 0$ satisfy the conditions*

$$\begin{aligned} s_1 b_u &< 1 \\ \frac{r_v}{r_u} &< \frac{1 - s_1 b_u}{1 + s_1 b_u}, \end{aligned}$$

then a stable limit cycle exists.

4. EXISTENCE OF SOLUTIONS LOCALLY IN TIME

In this section, we prove the existence of a unique weak solution of the system (1)-(6) up to a time $T > 0$. We make use of an iterative procedure instead of the classical approach via semigroup theory. Our iterative method allows a separate treatment of the two equations in each step. Bounds for the quadratic nonlinearities are obtained through regularity results and embedding theorems, while an exponential bound is obtained for the concentration of the inhibitor substance.

We confine ourselves to the case $S_u = 0$, when there is no saturation. The proof for the case $S_u > 0$ is analogous, the only difference being that for $S_u > 0$ the reaction function $f : \mathbb{R} \rightarrow \mathbb{R}$ of the Gierer-Meinhardt system (given by (3)) is required to be Lipschitz-continuous in u and bounded, allowing to obtain the necessary estimates in an easier way.

We consider the function spaces

$$(11) \quad X := L^\infty(0, T; H^1(\Omega)),$$

$$(12) \quad Y := \{u \in L^2(0, T; H^2(\Omega)) : u_t \in L^2(0, T; L^2(\Omega))\}.$$

Definition 4.1. A weak solution of (1), (2) with the boundary conditions (5) and the initial data (6) is a pair (u, v) of functions in $X \times X$, such that for all $\phi \in H^1(\Omega)$ a.e. in $[0, T]$ the following two equations are satisfied:

$$(13) \quad \langle u_t, \phi \rangle + \int_{\Omega} d_u \nabla u \nabla \phi d\mathbf{x} + \int_{\Omega} r_u u \phi d\mathbf{x} = \langle \hat{f}(u, v), \phi \rangle$$

$$(14) \quad \text{with } \hat{f}(u, v) := s_1 \left(\frac{u^2}{v} + b_u \right)$$

$$(15) \quad \langle v_t, \phi \rangle + \int_{\Omega} d_v \nabla v \nabla \phi d\mathbf{x} + \int_{\Omega} r_v v \phi d\mathbf{x} = \langle \hat{g}(u, v), \phi \rangle$$

$$(16) \quad \text{with } \hat{g}(u, v) := s_2 u^2 + b_v.$$

Theorem 4.1. Let $u_0, v_0 \in H^1(\Omega)$. Assume there is a constant $C_v \in \mathbb{R}$, such that

$$(17) \quad v_0(\mathbf{x}) \geq C_v > 0 \text{ a.s. in } \Omega.$$

Then there is a $T > 0$, such that the system (1), (2) with boundary conditions (5) and initial conditions (6) has a unique weak solution $(u, v) \in (X \times X) \cap (Y \times Y)$.

Remark 4.1. The condition (17) is necessary for treating the nonlinearity $1/v$ in the reaction function \hat{f} of the Gierer-Meinhardt system.

We set

$$T := \prod_{i=0}^5 T_i$$

for $T_i \leq 1$ to be defined in the following.

In order to prove Theorem 4.1, we construct a sequence $(u^m, v^m)_{m \in \mathbb{N}_0} \in (X \times X) \cap (Y \times Y)$ and show its convergence to the weak solution of the Gierer-Meinhardt problem.

Let $(u^0, v^0) \in (X \times X) \cap (Y \times Y)$ be the weak solution of

$$(18) \quad \frac{\partial u^0}{\partial t} - d_u \Delta u^0 + r_u u^0 = s_1 b_u$$

and

$$(19) \quad \frac{\partial v^0}{\partial t} - d_v \Delta v^0 + r_v v^0 = b_v$$

with boundary conditions (5) and initial conditions (6).

Further let $(u^m, v^m) \in (X \times X) \cap (Y \times Y)$ with $m \in \mathbb{N}$ be the weak solution of

$$(20) \quad \frac{\partial u^{m+1}}{\partial t} - d_u \Delta u^{m+1} + r_u u^{m+1} = \hat{f}(u^m, v^m)$$

and

$$(21) \quad \frac{\partial v^{m+1}}{\partial t} - d_v \Delta v^{m+1} + r_v v^{m+1} = \hat{g}(u^m, v^m)$$

with conditions (5), (6). The reaction functions \hat{f} and \hat{g} are given by (14) and (16). The existence and uniqueness of the functions $(u^m, v^m)_{m \in \mathbb{N}_0}$ in the sequence are guaranteed by the following

Lemma 4.1. [*Properties of the iteration sequence*]

(i) *The systems (18), (19) and (20), (21) with conditions (5), (6) possess unique weak solutions, and for each $m \in \mathbb{N}_0$ it holds*

$$(22) \quad u^m, v^m \in L^2(0, T; H^2(\Omega)) \cap L^\infty(0, T; H^1(\Omega))$$

$$(23) \quad u_t^m, v_t^m \in L^2(0, T; L^2(\Omega)).$$

(ii) *The functions u^m satisfy for each $m \in \mathbb{N}_0$ the estimate*

$$(24) \quad \|u^m\|_X^2 + \|u^m\|_{L^2(0, T; H^2(\Omega))} + \|u_t^m\|_{L^2(0, T; L^2(\Omega))} \leq 2C(\Omega, T) \|u_0\|_{H^1(\Omega)}^2.$$

(iii) *The functions v^m satisfy for each $m \in \mathbb{N}_0$ the estimate*

$$(25) \quad \|v^m\|_X^2 + \|v^m\|_{L^2(0, T; H^2(\Omega))} + \|v_t^m\|_{L^2(0, T; L^2(\Omega))} \leq C(\Omega, T) (\|u_0\|_{H^1(\Omega)}^2 + \|v_0\|_{H^1(\Omega)}^2).$$

(iv) *The functions v^m are for each $m \in \mathbb{N}_0$ bounded from below by*

$$(26) \quad v^m(t, \mathbf{x}) \geq C_v e^{-r_v t} \text{ for a.e. } \mathbf{x} \in \Omega \text{ and } t \in [0, T].$$

(v) *The functions u^m are for each $m \in \mathbb{N}_0$ bounded from below by*

$$(27) \quad u^m(t, \mathbf{x}) \geq C_u e^{-r_u t} \text{ for a.e. } \mathbf{x} \in \Omega \text{ and } t \in [0, T].$$

Proof of Lemma 4.1.

Induction start:

From the theory of linear parabolic equations (see e.g., [1]) it is well known that the system (5), (6), (18), (19) has a unique weak solution (u^0, v^0) with

$$u^0, v^0 \in L^2(0, T; H^1(\Omega)) \cap C(0, T; L^2(\Omega))$$

$$u_t^0, v_t^0 \in L^2(0, T; L^2(\Omega)).$$

Standard regularity theory yields the estimates

$$\|u^0\|_X^2 + \|u^0\|_{L^2(0, T; H^2(\Omega))} + \|u_t^0\|_{L^2(0, T; L^2(\Omega))} \leq C(\Omega, T) \left(T s_1^2 b_u^2 |\Omega| + \|u_0\|_{H^1(\Omega)}^2 \right)$$

and

$$\|v^0\|_X^2 + \|v^0\|_{L^2(0, T; H^2(\Omega))} + \|v_t^0\|_{L^2(0, T; L^2(\Omega))} \leq C(\Omega, T) \left(T b_v^2 |\Omega| + \|v_0\|_{H^1(\Omega)}^2 \right).$$

Upon setting

$$T_0 := \min \left\{ 1, \frac{\|u_0\|_{H^1(\Omega)}^2}{2s_1^2 b_u^2 |\Omega|}, \frac{\|u_0\|_{H^1(\Omega)}^2}{2b_v^2 |\Omega|} \right\},$$

we get

$$\begin{aligned} \|u^0\|_X^2 + \|u^0\|_{L^2(0,T;H^2(\Omega))} + \|u_t^0\|_{L^2(0,T;L^2(\Omega))} &\leq 2C(\Omega, T) \|u_0\|_{H^1(\Omega)}^2, \\ \|v^0\|_X^2 + \|v^0\|_{L^2(0,T;H^2(\Omega))} + \|v_t^0\|_{L^2(0,T;L^2(\Omega))} &\leq C(\Omega, T) (\|u_0\|_{H^1(\Omega)}^2 + \|v_0\|_{H^1(\Omega)}^2). \end{aligned}$$

The proof of property (26) for v^0 does not differ from the one for $m \in \mathbb{N}$ given below and is therefore omitted here.

Now all assertions of the Lemma for the case $m = 0$ are shown.

Induction hypothesis:

Assume the assertions of the lemma hold for an arbitrary $m \in \mathbb{N}_0$.

Inductive step:

We first show that $f(u^m, v^m) \in L^2(0, T; L^2(\Omega))$:

$$\begin{aligned} \int_0^T \left\| \hat{f}(u^m, v^m) \right\|_{L^2(\Omega)}^2 dt &= \int_0^T \left\| s_1 \frac{(u^m)^2}{v^m} + s_1 b_u \right\|_{L^2(\Omega)}^2 dt \\ &\stackrel{(26)}{\leq} \int_0^T \left(\frac{e^{rvt}}{C_v} s_1 \|(u^m)^2\|_{L^2(\Omega)} + s_1 b_u |\Omega|^{\frac{1}{2}} \right)^2 dt \\ &\leq \frac{2s_1^2}{C_v^2} \int_0^T e^{2rvt} \|(u^m)^2\|_{L^2(\Omega)}^2 dt + 2s_1^2 b_u^2 T_0 T_2 |\Omega| \\ &\leq \frac{2s_1^2}{C_v^2} \int_0^T e^{2rvt} \|u^m\|_{L^4(\Omega)}^4 dt + T_2 \|u_0\|_{H^1(\Omega)}^2 \\ &\leq \frac{2s_1^2 C^4}{C_v^2} e^{2r_v T} \int_0^T \|u_m\|_{H^1(\Omega)}^4 dt + T_2 \|u_0\|_{H^1(\Omega)}^2 \\ &\stackrel{(24)}{\leq} \frac{8s_1^2 C^4}{C_v^2} e^{2r_v T_2} C(\Omega, T)^2 T_1 T_2 \|u_0\|_{H^1(\Omega)}^4 dt + T_2 \|u_0\|_{H^1(\Omega)}^2. \end{aligned}$$

Now choose T_1 such that $T_1 C(\Omega, T)^2 \leq 1$ holds and set

$$T_2 := \min \left\{ \frac{1}{2}, \frac{1}{4r_v}, \frac{C_v^2}{16C^4 s_1^2 e^{r_v}} \|u_0\|_{H^1(\Omega)}^2 \right\},$$

which yields

$$\int_0^T \left\| \hat{f}(u^m, v^m) \right\|_{L^2(\Omega)}^2 dt \leq \|u_0\|_{H^1(\Omega)}^2 < \infty.$$

We next show that $g(u^m, v^m) \in L^2(0, T; L^2(\Omega))$:

$$\begin{aligned}
\int_0^T \|\hat{g}(u^m, v^m)\|_{L^2(\Omega)}^2 dt &= \int_0^T \|s_2(u^m)^2 + b_v\|_{L^2(\Omega)}^2 dt \\
&\leq \int_0^T \left(s_2 \|(u^m)^2\|_{L^2(\Omega)} + b_v |\Omega|^{\frac{1}{2}} \right)^2 dt \\
&\leq 2s_2^2 \int_0^T \|(u^m)^2\|_{L^2(\Omega)}^2 dt + 2b_v^2 T |\Omega| \\
&\stackrel{T \leq T_3}{\leq} 2C^4 s_2^2 \int_0^T \|u^m\|_{H^1(\Omega)}^4 dt + 2b_v^2 T_3 |\Omega| \\
&\stackrel{(24)}{\leq} 8C^4 s_2^2 C(\Omega, T)^2 T_1 T_3 \|u_0\|_{H^1(\Omega)}^4 + 2b_v^2 T_3 |\Omega| \\
&\leq \|u_0\|_{H^1(\Omega)}^2 < \infty,
\end{aligned}$$

where we denoted

$$T_3 := \min \left\{ 1, \frac{1}{16C^4 s_2^2 \|u_0\|_{H^1(\Omega)}^2}, \frac{\|u_0\|_{H^1(\Omega)}^2}{4b_v^2 |\Omega|} \right\}.$$

Now the linear theory yields the existence of a unique weak solution of (20), (21) with initial data (6) and boundary conditions (5). The solution (u^{m+1}, v^{m+1}) satisfies

$$\begin{aligned}
u^{m+1}, v^{m+1} &\in L^2(0, T; H^1(\Omega)) \cap C(0, T; L^2(\Omega)) \\
u_t^{m+1}, v_t^{m+1} &\in L^2(0, T; L^2(\Omega)),
\end{aligned}$$

and we have the estimates

$$\begin{aligned}
\|u^{m+1}\|_X^2 + \|u^{m+1}\|_{L^2(0, T; H^2(\Omega))}^2 + \|u_t^{m+1}\|_{L^2(0, T; L^2(\Omega))}^2 &\leq 2C(\Omega, T) \|u_0\|_{H^1(\Omega)}^2 \\
\|v^{m+1}\|_X^2 + \|v^{m+1}\|_{L^2(0, T; H^2(\Omega))}^2 + \|v_t^{m+1}\|_{L^2(0, T; L^2(\Omega))}^2 &\leq C(\Omega, T) (\|u_0\|_{H^1(\Omega)}^2 + \|v_0\|_{H^1(\Omega)}^2).
\end{aligned}$$

Now we only have to establish a lower bound for v^{m+1} . To do this, we define an auxiliary function w^{m+1} by $w^{m+1}(t, \mathbf{x}) := v^{m+1}(t, \mathbf{x}) - C_v e^{-r_v t}$. For this function it holds

$$\langle w_t^{m+1}(t), \phi \rangle + d_v \int_{\Omega} \nabla w^{m+1} \nabla \phi d\mathbf{x} + r_v \int_{\Omega} w^{m+1} \phi d\mathbf{x} = \langle \hat{g}(u^m, v^m), \phi \rangle.$$

For every non-negative $\phi \in H^1(\Omega)$, the right hand side is positive. Further, $w^{m+1}(\mathbf{x}, 0) \geq 0$, by construction. From the weak maximum principle, it follows that $w^{m+1} \geq 0$ a.e, yielding the lower bound $v^{m+1}(t, \mathbf{x}) \geq C_v e^{-r_v t}$. The proof of the corresponding property (27) for u^{m+1} is then analogous.

Now all assertions of the lemma are shown for $m + 1$ and this completes the induction and thus the proof. \square

Now we are able to prove Theorem 4.1.

Proof of Theorem 4.1.

Existence

We only have to show that the iterative sequence defined above is a Cauchy sequence. Then from the completeness of $H^1(\Omega)$ the existence of limiting functions u and v satisfying the equations (1), (2), (6) will follow.

Let $m \in \mathbb{N}$ be arbitrary. From (20) we get the estimate

$$\|u^{m+1} - u^m\|_X^2 \leq C(\Omega, T) \int_0^T \left\| \hat{f}(u^m, v^m) - \hat{f}(u^{m-1}, v^{m-1}) \right\|_{L^2(\Omega)}^2 dt.$$

For the right-hand side we further get (with C an adequate embedding constant)

$$\begin{aligned} & \int_0^T \left\| \hat{f}(u^m, v^m) - \hat{f}(u^{m-1}, v^{m-1}) \right\|_{L^2}^2 dt \\ &= s_1^2 \int_0^T \left\| \frac{(u^m)^2}{v^m} - \frac{(u^{m-1})^2}{v^{m-1}} \right\|_{L^2}^2 dt \\ &\leq 2s_1^2 \int_0^T \left\| \frac{(u^m)^2}{v^m} - \frac{u^m u^{m-1}}{v^m} \right\|_{L^2}^2 + \left\| \frac{u^m u^{m-1}}{v^m} - \frac{(u^{m-1})^2}{v^{m-1}} \right\|_{L^2}^2 dt \\ &\stackrel{(26)}{\leq} 2s_1^2 C_v^{-2} e^{2r_v T} \int_0^T \|u^m\|_{L^4}^2 \|u^m - u^{m-1}\|_{L^4}^2 dt \\ &\quad + 2s_1^2 \int_0^T \|u^{m-1}\|_{L^4}^2 \left\| \left(\frac{u^m}{v^m} - \frac{u^{m-1}}{v^{m-1}} \right)^2 \right\|_{L^2} dt \\ &\leq 2s_1^2 C^4 C_v^{-2} e^{2r_v T} \int_0^T \|u^m\|_{H^1}^2 \|u^m - u^{m-1}\|_{H^1}^2 dt \\ &\quad + C^2 2s_1^2 \int_0^T \|u^{m-1}\|_{H^1}^2 \left\| \left(\frac{u^m}{v^m} - \frac{u^{m-1}}{v^{m-1}} \right)^2 \right\|_{L^2} dt \\ &\leq 2s_1^2 C^4 C_v^{-2} e^{2r_v T_2} T \|u^m\|_X^2 \|u^m - u^{m-1}\|_X^2 \\ &\quad + 2s_1^2 C^2 \|u^{m-1}\|_X^2 \int_0^T \left\| \left(\frac{u^m}{v^m} - \frac{u^{m-1}}{v^{m-1}} \right)^2 \right\|_{L^2} dt \\ &\stackrel{(24)}{\leq} 4s_1^2 C(\Omega, T) C^4 C_v^{-2} e^{2r_v T_2} T \|u_0\|_{H^1}^2 \|u^m - u^{m-1}\|_X^2 \\ &\quad + 4s_1^2 C^2 C(\Omega, T) \|u_0\|_{H^1}^2 \int_0^T \left\| \left(\frac{u^m}{v^m} - \frac{u^{m-1}}{v^{m-1}} \right)^2 \right\|_{L^2} dt. \end{aligned}$$

For the last factor on the right hand side we have

$$\begin{aligned}
& \int_0^T \left\| \left(\frac{u^m}{v^m} - \frac{u^{m-1}}{v^{m-1}} \right)^2 \right\|_{L^2(\Omega)} dt \\
& \leq \int_0^T \left\| \left(\frac{u^m}{v^m} - \frac{u^m}{v^{m-1}} \right)^2 \right\|_{L^2(\Omega)} dt + \int_0^T \left\| \left(\frac{u^m}{v^{m-1}} - \frac{u^{m-1}}{v^{m-1}} \right)^2 \right\|_{L^2(\Omega)} dt \\
& \leq e^{4r_v T} C_v^{-4} \int_0^T \|u^m\|_{L^8(\Omega)}^2 \|v^m - v^{m-1}\|_{L^8(\Omega)}^2 dt \\
& \quad + e^{4r_v T} C_v^{-2} \int_0^T \|u^m - u^{m-1}\|_{L^8(\Omega)}^2 dt \\
& \leq C^4 C_v^{-4} e^{4r_v T} \int_0^T \|u^m\|_{H^1(\Omega)}^2 \|v^m - v^{m-1}\|_{H^1(\Omega)}^2 dt \\
& \quad + C^2 C_v^{-2} e^{4r_v T} \int_0^T \|u^m - u^{m-1}\|_{H^1(\Omega)}^2 dt \\
& \leq C^2 \frac{1}{C_v^2} e^{4r_v T_2} T \left(C^2 C_v^2 \|u^m\|_X^2 \|v^m - v^{m-1}\|_X^2 + \|u^m - u^{m-1}\|_X^2 \right) \\
& \stackrel{(24)}{\leq} 2C^4 \frac{1}{C_v^4} C(\Omega, T) e^{4r_v T_2} T \|u_0\|_{H^1(\Omega)}^2 \|v^m - v^{m-1}\|_X^2 + C^2 \frac{1}{C_v^2} e^{4r_v T_2} T \|u^m - u^{m-1}\|_X^2.
\end{aligned}$$

From (21) we get

$$\|v^{m+1} - v^m\|_X^2 \leq C(\Omega, T) \int_0^T \|\hat{g}(u^m, v^m) - \hat{g}(u^{m-1}, v^{m-1})\|_{L^2(\Omega)}^2 dt.$$

For the right hand side we further estimate

$$\begin{aligned}
& \int_0^T \|\hat{g}(u^m, v^m) - \hat{g}(u^{m-1}, v^{m-1})\|_{L^2}^2 dt \\
& = s_2^2 \int_0^t \|(u^m - u^{m-1})^2\|_{L^2(\Omega)}^2 dt \\
& \leq s_2^2 C^4 \int_0^T \|u^m - u^{m-1}\|_{H^1(\Omega)}^2 \|u^m + u^{m-1}\|_{H^1(\Omega)}^2 dt \\
& \leq s_2^2 C^4 \|u^m - u^{m-1}\|_X^2 \int_0^T \|u^m + u^{m-1}\|_{H^1(\Omega)}^2 dt \\
& \leq 2s_2^2 C^4 \|u^m - u^{m-1}\|_X^2 \int_0^T \left(\|u^m\|_{H^1(\Omega)}^2 + \|u^{m-1}\|_{H^1(\Omega)}^2 \right) dt \\
& \leq 2s_2^2 C^4 T \|u^m - u^{m-1}\|_X^2 \left(\|u^m\|_X^2 + \|u^{m-1}\|_X^2 \right) \\
& \stackrel{(24)}{\leq} 8s_2^2 C^4 C(\Omega, T) T \|u_0\|_{H^1}^2 \|u^m - u^{m-1}\|_X^2.
\end{aligned}$$

Summarising the previous estimates we obtain

$$\begin{aligned}
& \|u^{m+1} - u^m\|_X^2 + \|v^{m+1} - v^m\|_X^2 \\
& \leq 8(s_1^2 C_v^2 e + s_2^2) C^4 \|u_0\|_{H^1}^2 C(\Omega, T)^2 \kappa T_1 T_5 \|u^m - u^{m-1}\|_X^2 \\
& \quad + 8s_1^2 C^6 C_v^4 e \|u_0\|_{H^1}^4 C(\Omega, T)^3 \kappa T_1 T_4 T_5 \|v^m - v^{m-1}\|_X^2 \\
& \leq 8(s_1^2 C_v^2 e + s_2^2) C^4 \|u_0\|_{H^1}^2 \kappa T_5 \|u^m - u^{m-1}\|_X^2 \\
& \quad + 8s_1^2 C^6 C_v^4 e \|u_0\|_{H^1}^4 \kappa T_5 \|v^m - v^{m-1}\|_X^2,
\end{aligned}$$

where T_4 has been chosen such that $T_4 C(\Omega, T) \leq 1$.

With

$$T_5 := \min \left\{ 1, \frac{1}{16(s_1^2 C_v^2 e + s_2^2) C^4 \|u_0\|_{H^1}^2}, \frac{1}{16s_1^2 C^6 C_v^4 e \|u_0\|_{H^1}^4} \right\},$$

we finally get

$$(28) \quad \|u^{m+1} - u^m\|_X^2 + \|v^{m+1} - v^m\|_X^2 \leq \frac{1}{2} \left(\|u^m - u^{m-1}\|_X^2 + \|v^m - v^{m-1}\|_X^2 \right).$$

Thus, (u^m, v^m) is a Cauchy sequence in $X \times X$, from which the existence of a weak solution of (1)-(6) follows. \square

Uniqueness

To prove the uniqueness of the solution assume that (u_1, v_1) and (u_2, v_2) are weak solutions of (1)-(6). Due to (28), it follows that

$$(29) \quad \|u_1 - u_2\|_X^2 + \|v_1 - v_2\|_X^2 \leq \frac{1}{2} \left(\|u_1 - u_2\|_X^2 + \|v_1 - v_2\|_X^2 \right).$$

Therefore, $(u_1, v_1) = (u_2, v_2)$ in $X \times X$, i.e. the weak solution of (1)-(6) is unique. \square

Regularity of the solution

From (22) and (23) we know that (u^m, v^m) is uniformly bounded in $Y \times Y$ with respect to m and the embedding of Y in $L^2(0, T; H^1(\Omega))$ is compact.

Passing to the limit for $m \rightarrow \infty$, we obtain $(u, v) \in Y \times Y$. \square

5. GLOBAL EXISTENCE OF SOLUTIONS

In this section we prove that the solution of the Gierer-Meinhardt system exists for all times $t \geq 0$, provided that the initial data are appropriately bounded.

To this end, we apply the method of invariant regions as outlined in [11]. First we recall for convenience some general results from this work, which are then used to prove the existence of an invariant region for the Gierer-Meinhardt system.

In the following we will need the function spaces

$$\begin{aligned} BC(\mathbb{R}^N) &:= \{ \text{bounded, uniformly continuous functions on } \mathbb{R}^N \} \\ BC_0(\mathbb{R}^N) &:= \{ w \in BC : |w(\mathbf{x})| \rightarrow 0 \text{ f\"ur } |\mathbf{x}| \rightarrow \infty \}. \end{aligned}$$

The method of invariant regions can be applied to systems of the form

$$(30) \quad \frac{\partial u}{\partial t} = D\Delta u + f(u) \quad \text{for all } (\mathbf{x}, t) \in \Omega \times \mathbb{R}_+$$

with initial data

$$(31) \quad u(0, \mathbf{x}) = u_0(\mathbf{x}), \quad \mathbf{x} \in \Omega.$$

Here Ω is an open subset of \mathbb{R}^N , $D \in \mathbb{R}^{m \times m}$ is a positive definite matrix, u is an m -dimensional vector, and f is a smooth mapping from U to \mathbb{R}^m , where U is an open subset of \mathbb{R}^m .

Following [11], we state the definition of an invariant region for (30):

Definition 5.1. (*Definition 14.5, [11]*)

A closed subset $\Sigma \subset \mathbb{R}^m$ is called a (positive) **invariant region** for the local solution of (30), if every solution $u(\mathbf{x}, t)$ with initial data and boundary data in Σ stays in Σ for all $\mathbf{x} \in \Omega$ and $t \in [0, \delta)$.

In the case where the diffusion matrix D is diagonal, the following criterion allows to obtain a special type of invariant regions, the so called *invariant rectangles*. The theorem is a combination of Corollary 14.8(a) and Theorem 14.11 in [11].

Theorem 5.1. *If D is a diagonal matrix, then every set of the form*

$$\Sigma = \bigcap_{i=1}^m \{ u : a_i \leq u_i \leq b_i \}$$

is invariant for (30), provided that for $i = 1, \dots, m$ the conditions

$$(32) \quad \nabla_u(a_i - u_i) \cdot f|_{u_i=a_i} \leq 0 \text{ in } \Sigma,$$

$$(33) \quad \nabla_u(u_i - b_i) \cdot f|_{u_i=b_i} \leq 0 \text{ in } \Sigma$$

are satisfied.

The value of invariant regions for the proof of global existence stems from the following result [11]:

Theorem 5.2. *If a bounded invariant region exists for the system (30) with initial data $u_0 \in BC_0$ and $u_0(\mathbf{x}) \in \Sigma$ holds for all $\mathbf{x} \in \Omega$, then the solution of this system exists for all $t \geq 0$.*

We are now going to apply the theory outlined above to the special case of the Gierer-Meinhardt system.

In matrix notation the GM-System (1), (2) with reaction functions (3) and (4) reads

$$(34) \quad \begin{pmatrix} u_t \\ v_t \end{pmatrix} = \begin{pmatrix} d_u & 0 \\ 0 & d_v \end{pmatrix} \begin{pmatrix} \Delta u \\ \Delta v \end{pmatrix} + \begin{pmatrix} s_1 \left(\frac{u^2}{v(1+S_u u^2)} + b_u \right) - r_u u \\ s_2 u^2 + b_v - r_v v \end{pmatrix}.$$

As in the proof of local existence we restrict ourselves to the case $S_u = 0$. As before, we assume initial data (6) and homogeneous Neumann boundary conditions (5).

We set

$$\Sigma = \{(u, v) : 0 \leq u \leq \alpha, \beta \leq v \leq \gamma\}.$$

Our aim is to determine the constants $\alpha, \beta, \gamma \in \mathbb{R}$ ensuring the invariance of Σ for the Gierer-Meinhardt system. To do this, we define

$$V = \left[s_1 \left(\frac{u^2}{v} + b_u \right) - r_u u, s_2 u^2 + b_v - r_v v \right]$$

and get

- For $G = -u$:

$$\begin{pmatrix} G_u \\ G_v \end{pmatrix} \cdot V|_{u=0} = -s_1 b_u \leq 0 \text{ in } \Sigma, \text{ therefore } 0 \leq u.$$

- For $G = \beta - v$:

Upon setting $\beta = b_v/r_v$, we get

$$\begin{pmatrix} G_u \\ G_v \end{pmatrix} \cdot V|_{v=\beta} = -s_2 u^2 - b_v + r_v = -s_2 u^2 \leq 0 \text{ in } \Sigma, \text{ therefore } \beta \leq v.$$

- For $G = u - \alpha$:

$$\begin{pmatrix} G_u \\ G_v \end{pmatrix} \cdot V|_{u=\alpha} = s_1 \left(\frac{\alpha^2}{v} + b_u \right) - r_u \alpha \stackrel{!}{\leq} 0 \text{ in } \Sigma.$$

This condition leads with $\frac{b_v}{r_v} \leq v$ to an inequality for α

$$\alpha^2 - \frac{r_u b_v}{s_1 r_v} + b_u \frac{b_v}{r_v} \alpha \leq 0.$$

In order to get real solutions for this quadratic inequality, we have to impose the additional constraint

$$\frac{r_u^2 b_v}{s_1^2 r_v} \geq 4b_u$$

on the parameters of the system. Since we want the invariant region Σ to be as large as possible, we choose α to be

$$(35) \quad \alpha = \frac{1}{2} \left[\frac{r_u b_v}{s_1 r_v} + \sqrt{\frac{r_u^2 b_v^2}{s_1^2 r_v^2} - 4b_u \frac{b_v}{r_v}} \right].$$

For this choice of α it holds that $u \leq \alpha$ on Σ .

- For $G = v - \gamma$:

$$\begin{pmatrix} G_u \\ G_v \end{pmatrix} \cdot V|_{v=\gamma} = s_2 u^2 + b_v - r_v \gamma \stackrel{!}{\leq} 0 \text{ in } \Sigma.$$

Since $u \leq \alpha$, this condition is fulfilled for

$$\gamma \geq \frac{1}{r_v} [s_2 \alpha^2 + b_v].$$

Inserting α from (35) leads to

$$\gamma \geq \frac{s_2}{4r_v} \left[\frac{r_u b_v}{s_1 r_v} + \sqrt{\frac{r_u^2 b_v^2}{s_1^2 r_v^2} - 4b_u \frac{b_v}{r_v}} \right]^2 + \frac{b_v}{r_v}.$$

For this choice of γ we then have $v \leq \gamma$ on Σ .

With the choice of parameters above, Theorem 5.1 yields that Σ is invariant for the Gierer-Meinhardt system.

We can now employ Theorem 5.2 to obtain

Theorem 5.3. *If the initial data $(u_0, v_0) \in BC_0$ satisfies $(u_0(\mathbf{x}), v_0(\mathbf{x})) \in \Sigma$ for every $\mathbf{x} \in \Omega$ and if*

$$(36) \quad \frac{r_u^2 b_v}{s_1^2 r_v} \geq 4b_u,$$

the corresponding solution of the GM-system exists for all times $t \geq 0$.

6. NUMERICAL SIMULATIONS

In this chapter we perform numerical simulations for the Gierer-Meinhardt system. After a short outline of the discretization methods we present the simulation results.

For the spatial discretization, we use the finite element method with piecewise linear basis functions. To do this, we consider the projection of (13) and (15) onto a finite dimensional subspace $V_m \subset H^1(\Omega)$. Let (ϕ_1, \dots, ϕ_m) ($m \in \mathbb{N}$) be the linear basis functions for V_m . Then the discretized problem consists in finding

functions $(u(t), v(t)) \in L^2(0, T; V_m) \times L^2(0, T; V_m)$ satisfying the system of ordinary differential equations

$$(37) \quad Bu_t + d_u Mu(t) + r_u Bu(t) = b_i^u(t)$$

$$(38) \quad Bv_t + d_v Mv(t) + r_v Bv(t) = b_i^v(t),$$

with the matrices $B \in \mathbb{R}^{m \times m}$ and $M \in \mathbb{R}^{m \times m}$ given by

$$(39) \quad M_{j,k} = \int_{\Omega} \nabla \phi_j \nabla \phi_k \quad B_{j,k} = \int_{\Omega} \phi_j \phi_k$$

and the right-hand sides $b^u \in \mathbb{R}^m$ and $b^v \in \mathbb{R}^m$ given by

$$(40) \quad b_i^u(t) = \int_{\Omega} \hat{f}(u(t), v(t)) \phi_i \quad b_i^v(t) = \int_{\Omega} \hat{g}(u(t), v(t)) \phi_i.$$

This system has now to be discretized in time. To do this, we use an implicit discretization for the term representing the Laplacian and an explicit discretization of the reaction functions. This is the so-called IMEX method (see e.g., [9]), which avoids oscillations and the occurrence of negative values for the chemical concentrations that are observed for example in the explicit Euler method. Compared with fully implicit methods, this approach has the advantage that we do not have to solve a system of nonlinear equations which would be far more time consuming. The fully discretized system now reads

$$\begin{aligned} (B + \Delta t d_u M)u(t + \Delta t) &= Bu(t) - \Delta t r_u Bu(t) + \Delta t b_i^u(t) \\ (B + \Delta t d_v M)v(t + \Delta t) &= Bv(t) - \Delta t r_v Bv(t) + \Delta t b_i^v(t). \end{aligned}$$

Here Δt is the size of the timestep, which has to be chosen small enough for the scheme to be stable.

Remark 6.1. *The iterative method employed for showing the existence of a solution to the coupled activator-inhibitor system can also be used to perform numerical simulations. Its convergence has already been proved in Section 4. This natural approach is however manifestly more computer intensive than the finite element method, therefore we preferred the latter for the numerical simulations in this section.*

We first simulate spatial patterns arising from the Turing-instability.

6.1. Patterns due to the Turing instability. We first consider the parameter set

$$(41) \quad \begin{pmatrix} r_u = 0.02 & s_1 = 0.02 & d_u = 0.01 & b_u = 0.03 & S_u = 0.0 \\ r_v = 0.06 & s_2 = 0.02 & d_v = 0.4 & b_v = 0.1072 & \end{pmatrix}$$

The formation of patterns by the mechanism of the Turing instability requires a perturbation of the steady state of the activator. For the Gierer-Meinhardt system with parameters (41), the spatially homogeneous steady state is given by $(u_s, v_s) \approx (0.0305, 1.7870)$.

It is easy to check that the condition (36) for the global existence of the solution is satisfied for (41). The invariant region Σ is then given by

$$(42) \quad \alpha = 1.7561 \quad \beta = 1.7867 \quad \gamma \geq 2.3720.$$

As initial distributions of the activator, respectively of the inhibitor we choose

$$(43) \quad u_0(x) = u_s + 0.001\xi(x) \text{ and } v_0(x) = v_s,$$

where $\xi(x)$ denotes a field of independent normal distributed random numbers. The initial values u_0 and v_0 then lie in the invariant region given by (42). The striped pattern obtained via computer simulations is shown in Figure 1. Here every point where the concentration of activator is above the steady state is coloured in black, while all other points were left white. The figure also shows an actual shell exhibiting the simulated pattern¹.

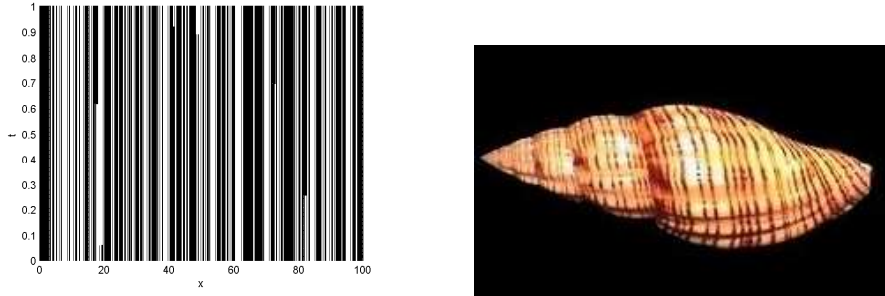


FIGURE 1. Left: For the parameters (41), the Gierer-Meinhardt system exhibits stripes parallel to the direction of growth. Right: pattern on *Lyria planicostata taiwanica*.

The influence of the saturation parameter of the activator is shown in the following pictures. For the left of Figure 2 we have set $S_u = 0.01$, while for the right part the saturation has been set to $S_u = 0.1$. The other parameters remained unchanged.

We observe that an increase in the saturation has scarcely an effect on the stripe pattern. It is not possible to observe any qualitative effects of the variation of this parameter on the picture.

We next examine two further choices of parameters, namely

$$(44) \quad \begin{pmatrix} r_u = 0.2 & s_1 = 0.2 & d_u = 0.01 & b_u = 0.3 & S_u = 0.0 \\ r_v = 0.6 & s_2 = 0.2 & d_v = 0.4 & b_v = 0.8200 & \end{pmatrix}$$

and

$$(45) \quad \begin{pmatrix} r_u = 0.002 & s_1 = 0.002 & d_u = 0.01 & b_u = 0.003 & S_u = 0.0 \\ r_v = 0.006 & s_2 = 0.002 & d_v = 0.4 & b_v = 0.1001 & \end{pmatrix}.$$

¹This Picture was taken from <http://www.specimenshells.net/1553.htm>.

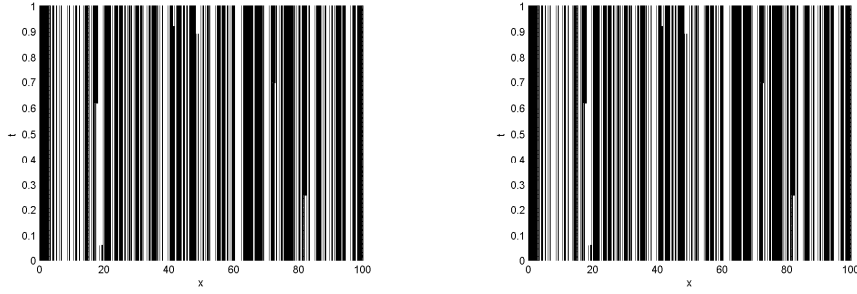


FIGURE 2. Left: pattern after the saturation has been increased to $S_u = 0.01$. Right: pattern after the saturation has been increased to $S_u = 0.1$.

We choose the initial distributions to be $u_0(\mathbf{x}) = 0.309 + 0.01\xi(\mathbf{x})$, $v_0(\mathbf{x}) = 13.6981$ for (44) and $u_0(\mathbf{x}) = 0.003 + 0.0001\xi(\mathbf{x})$, $v_0(\mathbf{x}) = 1.6679$ for (45).

The invariant Region Σ for (44) is given by

$$(46) \quad \alpha = 13.6366 \quad \beta = 13.6667 \quad \gamma \geq 18.2122,$$

and for (45) by

$$(47) \quad \alpha = 1.6373 \quad \beta = 1.6679 \quad \gamma \geq 2.2136.$$

The results in each case are shown in Figure 3.

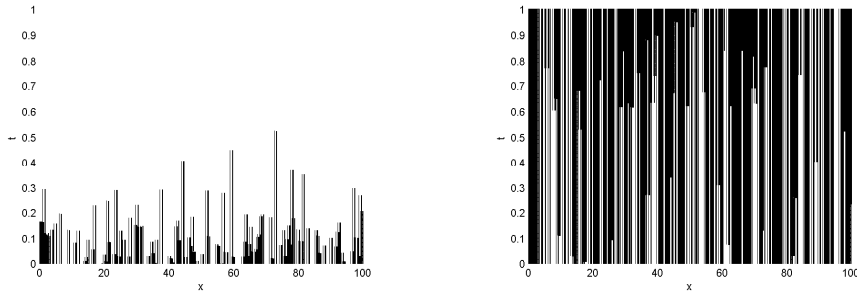


FIGURE 3. Left: pattern for the parameter set (44). Right: pattern for the parameters in (45)

In the left part of Figure 3 it can be noticed that for the set of parameters (44) the stripes thin out as time passes and finally dissolve completely. In this case, none of the stripes continues until the final time $T = 1$. The opposite effect can be obtained by choosing the parameters as (45). As can be observed in the right part of Figure 3, in this case the stripes thicken while time passes.

We conclude this section with the results for the (nondimensionalised) two dimensional system with parameters

$$(48) \quad d = 100 \quad a = 0 \quad b = 0.67 \quad c = 0 \quad \gamma = 7.5 \quad S_u = 0.3.$$

As initial distributions we choose

$$(49) \quad u_0(x) = u_s + 0.001\xi(\mathbf{x}) \text{ and } v_0(\mathbf{x}) = v_s,$$

where $(u_s, v_s) = (1.0911, 1.1912)$ denotes the homogeneous steady state of (7)-(10) with the parameters given by (48).

We choose the spatial domain to be the unit square $[0, 1] \times [0, 1]$. The right part of Figure 4 shows the emerging pattern, while the left part ² shows an example for the occurrence of this pattern in nature.

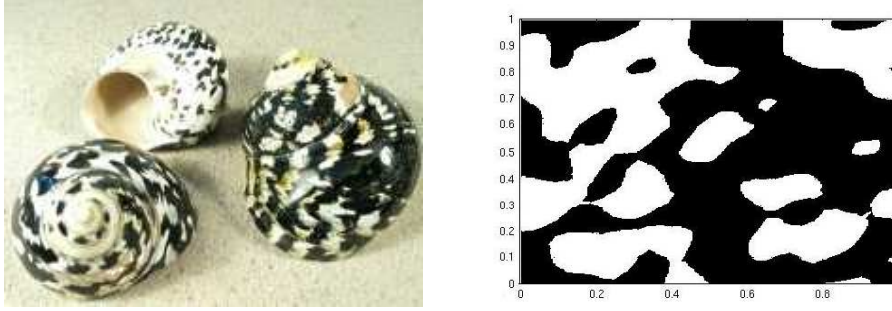


FIGURE 4. Left: spot-like pattern on *Cittarium pica*. Right: computer simulation.

6.2. Patterns due to temporal oscillations. We now choose the following parameters:

$$(50) \quad \begin{pmatrix} r_u = 0.5 & s_1 = 1 & d_u = 0.1 & b_u = 0.3 & S_u = 0.0 \\ r_v = 0.3 & s_2 = 0.05 & d_v = 0.8 & b_v = 0.0 & \end{pmatrix}.$$

In Figure 5, the temporal evolution of the concentration field of the activator for this set of parameters is shown. In the case of temporal oscillations, it is no longer meaningful to regard the equilibrium concentration of the activator as a threshold for the onset of pigment production. Therefore, the pictures in this section show the respective concentration field of the activator instead of the black and white pattern as in the last subsection. Times of high activator concentration correspond to phases of pigment production. To allow for a comparison with patterns in nature, the right part of the figure shows a specimen with the corresponding stripe pattern.

For the next figure we varied again the saturation of activator while keeping the values of the other parameters.

As can be seen, an increase in saturation leads to a lower maximum value of the activator concentration. After some time, the concentration of activator passes to a constant state.

²This picture was taken from www.trockenaquaristik.de.

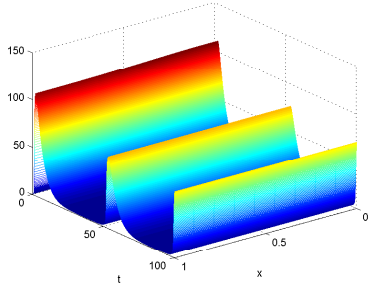


FIGURE 5. Left: concentration of activator for the parameter set (50). Right: pattern on *Amoria ellioti*.

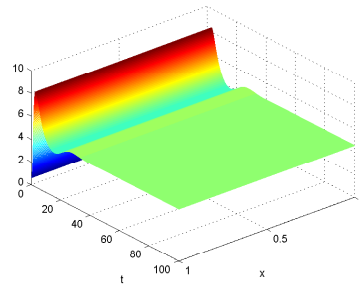
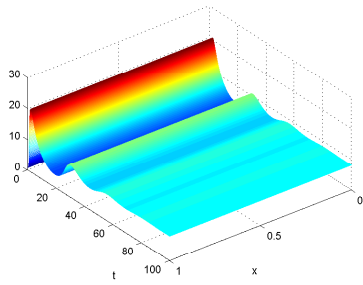


FIGURE 6. Left: concentration of activator for $S_u = 0.01$. Right: concentration of activator for $S_u = 0.1$.

The results for the parameters

$$(51) \quad \begin{pmatrix} r_u = 5 & s_1 = 10 & d_u = 0.1 & b_u = 3 & S_u = 0.0 \\ r_v = 3 & s_2 = 0.5 & d_v = 0.8 & b_v = 0.0 & \end{pmatrix}$$

are shown in the left part of Figure 7, while the right part shows the results for

$$(52) \quad \begin{pmatrix} r_u = 0.05 & s_1 = 0.1 & d_u = 0.1 & b_u = 0.03 & S_u = 0.0 \\ r_v = 0.03 & s_2 = 0.005 & d_v = 0.8 & b_v = 0.0 & \end{pmatrix}.$$

As can be seen in Figure 7, the frequency of the oscillations is noticeably increased by the choice of parameters (51) in comparison to (50). The concentration at the peaks increases faster and declines more rapidly. For the parameters (52), the exactly opposite effect can be observed.

7. CONCLUSIONS

We studied in this paper a reaction-diffusion system introduced by Gierer and Meinhardt (1972) to model the interaction of activator and inhibitor concentrations conditioning pattern formation on seashells. We gave a new, simple proof for the

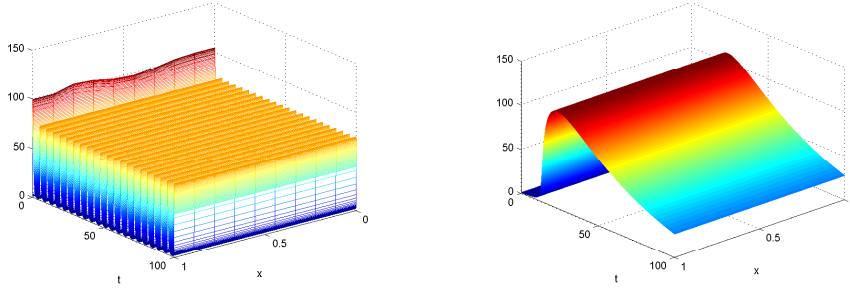


FIGURE 7. Left: activator field for the parameter set (51). Right: activator field for the set (52).

existence and uniqueness of the solution to this system and performed numerical simulations.

First, we proved the existence of a unique weak solution locally in time, with the aid of an iterative approach, unlikely the usual proof via semigroups of operators. This idea has already been used in a different context in [12] in order to show the existence of a highly nonlinear steady-state fluid-elastic structure interaction problem. It allows the system to be decoupled, offering thus the possibility of handling separately the equations for the activator, respectively the inhibitor. Moreover, it facilitates the estimation of the quadratic nonlinearities via classical embedding theorems and also leads to an exponential bound for the inhibitor concentration. The positivity of the solution is ensured as well.

Further, we have shown the global existence of the solution to the activator-inhibitor system upon using the intuitive and elegant method of invariant regions outlined in [11]. Through its geometrical nature, this approach also fastens up to the qualitative analysis of the system. The main issue was thereby to find an invariant region for the Gierer-Meinhardt system.

Performing the numerical simulations has shown that there is a minor influence of saturation on the striped space patterns, whereas higher saturation for time patterns leads to fast transition to a constant state. A uniform variation of the reaction parameters under constant diffusion rates has a large influence on the evolution of the stripes' width in the space-time patterns. For time oscillating patterns such variations lead to frequency changes.

Throughout this paper we assumed that the domain of interest was not moving in time. Space-time patterns similar to those observed on real seashells have been obtained even with this simplification (see Section 6), however considering time-varying domains would allow to account for the growth of the shells. This seems to be a nontrivial issue, at least from the viewpoint of mathematical analysis. While there are some numerical simulations for growing domains (see e.g.,

[6]), there are by our knowledge no results concerning existence and regularity for solutions to such problems.

We have considered here a pure deterministic system for modeling pattern formation, however the respective biochemical processes are by their nature random; their deterministic description relies on several assumptions, like e.g., a high enough number of molecules involved and a homogeneous medium. The parameters of the system are actually influenced by the environment, which can infer highly fluctuations. We will study these issues in the framework of a stochastic version of the Gierer-Meinhardt system in a forthcoming paper.

REFERENCES

- [1] L.C. Evans, **Partial Differential Equations**. AMS, 1998.
- [2] A. Gierer, H. Meinhardt, *A theory of biological pattern formation*, Kybernetik 12 (1972) 30-39.
- [3] H. Jiang, *Global existence of solutions of an Activator-Inhibitor System*. Disc. and Cont. Dyn. Sys. 14, 737-751 (2006).
- [4] M.I. Granero-Porati, A. Porati, *Temporal Organization in a morphogenetic field.*, J. Math. Biology 20, 153-157 (1984).
- [5] H. Meinhardt, **The Algorithmic Beauty of Seashells**, Springer, 2003.
- [6] H. Meinhardt, M. Klingler, *A model for pattern formation on the shells of molluscs*, J. Theor. Biol 126 (1987) 63-69.
- [7] J.D. Murray, **Mathematical Biology II**. Springer, 2003.
- [8] F. Rothe, **Global Solutions of Reaction-Diffusion Systems**. Lecture Notes in Math. 1072, Springer-Verlag (1984).
- [9] S. J. Ruuth, *Implicit-explicit methods for reaction-diffusion problems in pattern formation*, J. Math. Biol. 34 (1995) 148-176.
- [10] L.A. Segel, J.L. Jackson, *Dissipative structure: an explanation and an ecological example*, J. Theor. Biol. 37 (1972) 545-549.
- [11] J. Smoller, **Schock Waves and Reaction-Diffusion Equations**. Springer, 1994.
- [12] C. Surulescu, *On the stationary interaction of a Navier-Stokes fluid with an elastic tube wall*, Applicable Analysis 86 (2007) 149 - 165.
- [13] A.M. Turing, *The chemical basis of morphogenesis*. Phil Trans. Roy. Soc. London B 237, 37 (1952).
- [14] J. Wei, M. Winter, *Spikes for the two-dimensional Gierer-Meinhardt system: the weak coupling case*. J. Nonlinear Sci. 11(6), 415-458 (2001).
- [15] J. Wei, M. Winter, *Spikes for the Gierer-Meinhardt system in two dimensions: the strong coupling case*. J. Differential Equations, 178(2), 478-518 (2002).

Jan Kelkel
Pfaffenwaldring 57
70569 Stuttgart
Germany
E-Mail: jan.kelkel@mathematik.uni-stuttgart.de

Christina Surulescu
Pfaffenwaldring 57
70569 Stuttgart
Germany
E-Mail: christina.surulescu@ians.uni-stuttgart.de
WWW: <http://www.ians.uni-stuttgart.de/LstAngMath/Surulescu/>

Erschienenene Preprints ab Nummer 2008/001

Komplette Liste: <http://preprints.ians.uni-stuttgart.de>

- 2008/001 *Perfahl, H., Sändig, A.-M.:* A Continuum-Mechanical Approach to Avascular Solid Tumor Growth
- 2008/002 *Giesselmann, J.:* A convergence result for finite volume schemes on 2-dimensional Riemannian manifolds
- 2008/003 *Rohde, C., Surulescu, C.:* Mathematische Modellierung und Analyse von biologischen Prozessen
- 2008/004 *Lalegname, A., Sändig, A.-M., Sewell, G.:* Analytical and numerical treatment of a dynamic crack model
- 2008/005 *Kettemann, A.:* A mathematical model for mesenchymal and chemosensitive cell dynamics in tissue networks
- 2008/006 *Kelkel, J., Surulescu, C.:* Global existence and numerical simulations for a reaction-diffusion system modeling pattern formation on seashells